Acta Cryst. (1962). **15**, 337

Electron Density and Thermal Effects in Alpha Quartz**

BY R. A. YOUNG*† AND BEN POST

Polytechnic Institute of Brooklyn, Brooklyn 1, *N.Y., U.S.A.*

(*Received* 27 *April* 1960 *and in revised form* 22 *May* 1961)

A detailed analysis has been made of atomic positional coordinates and thermal motions in α-quartz. Complete data in three dimensions were obtained at room temperature using filtered Mo K radiation; ($hk0$) and ($00l$) reflections were also measured at 223 and 155 °K. Intensities were measured with a scintillation counter. Fourier and least squares techniques were used to determine positional coordinates and the magnitude and orientation of atomic thermal ellipsoids.

Data previously reported by Brill *et al.* (1939, 1942) have been refined by least squares methods and the new results have been found to be in good agreement with ours. The temperature dependence of the atomic coordinates and of the thermal parameters have been investigated by least squares analyses of data obtained at different temperatures and by direct comparison of electron density maps based on room and low temperature data. The applicability of the Debye approximation to the thermal data for α-quartz has also been investigated.

Bond lengths at room temperature are: Si–O: 1·603 ± 0·003 Å and 1·611 ± 0·002 Å. The Si–O–Si angle is 143·9°. Two of the four tetrahedral O–Si–O angles are close to 109°; the others are 110°.

1. Introduction

Alpha-quartz occurs with either of the enantiomorphically related space groups, $P3_112$ or $P3_212$. There are three formula weights per unit cell. The cell dimensions, as given by Bradley & Jay (1933), are:

$$a = 4{\cdot}9128 \pm 0{\cdot}00005,\ c = 5{\cdot}4042 \pm 0{\cdot}0001\ \text{Å}\ .$$

The positional parameters to be determined are, u, the distance from the threefold axis to the silicon atom, and the x, y, and z coordinates of one oxygen atom.

Brill *et al.* (1939, 1942) investigated α-quartz by Fourier methods, using room temperature ($h0{\cdot}l$) data gathered with an ionization chamber. The crystal specimens were slabs of natural milk quartz. Detailed comparisons of our results with Brill's have been made, in part by refinement of their data, and will be discussed later.

2. Experimental

All of our specimens were prepared from one of two clear, well-formed, single crystals of synthetic quartz supplied by Dr E. Wood of the Bell Telephone Laboratories. The crystals were about two centimeters long and three to four millimeters in hexagonal cross section. Except for a few regions where obvious flaws existed, the crystals extinguished sharply in polarized light. The flamed portions were easily removed. Spectrographic analysis of the sample material showed less than 0·0001% Be, <0·01% Mg, <0·001% Fe, <0·001% Cu, and <0·1% Ca.

Quartz is subject to two types of twinning: (*a*) optical, or Brazilian, and (*b*) electrical, or Dauphiné. Since the specimens extinguished sharply between crossed Nicols and well-formed rings were found in their optic figures, Brazilian twinning was considered to be absent.

Dauphiné twinning cannot be detected by means of polarizing optics. Etch tests and careful icing of the specimen do make it possible to detect a twin boundary at the surface of a crystal; when twinning is present a line forms at the twin boundary. No such line was found on icing of our specimens but this did not preclude the possibility that there were twins wholly included in the main crystal.

It can be shown that the effect of Dauphiné twinning is to make a reciprocal lattice point which is equivalent to the ($hk{\cdot}l$) of the rotated twin occur at the position of ($hk{\cdot}\bar{l}$) of the unrotated twin. Comparisons of observed and calculated values of $|F_{hk\cdot l}|^2$ and $|F_{hk\cdot\bar{l}}|^2$, and of the sums $[|F_{hk\cdot l}|^2 + |F_{hk\cdot\bar{l}}|^2]$ led us to conclude that Dauphiné twinning was absent from our crystals.

The crystals were ground to effectively spherical shapes (from 0·3 to 0·7 mm. in diameter). In no case did any diameters of the spheroids used deviate from the diameters of the equivalent spheres by more than 0·05 mm.

X-ray measurements were made with a scintillation counter mounted on a Weissenberg camera base. Filtered molybdenum radiation was used. Stability and linearity in the overall X-ray generation and detection apparatus were maintained to within about 1%. The apparatus and technique used to cool the crystals have been described previously (Post, Schwartz & Fankuchen (1951)).

---

* Now at Engineering Experiment Station, Georgia Institute of Technology, Atlanta 13, Georgia.

† Based on Dissertation for Ph.D. in Physics, The Polytechnic Institute of Brooklyn (1959).

** This work was supported in part by the Office of Naval Research.

Intensity data were determined primarily from measurements of peak heights, as described below. Results were reproducible to within 1% for all but the weakest reflections. One illustrative measure of reproducibility was obtained by measurement of twelve peaks at times one week apart. The goniometer had been removed and replaced in the interim and the crystal was necessarily realigned. The mean deviation from the mean was $1\frac{1}{4}$%.

Background was measured by rotating the crystal 3 to 5° from the original setting. An additional measurement was then made $\frac{1}{2}$° further from the peak to make certain that there was no significant contribution from the 'tails' of the peaks.

The intensities of all 309 independent reflections for which $\sin\theta/\lambda < 1{\cdot}4$ were measured using one crystal. Intensities of 32 ($hk{\cdot}0$) reflections and of the (00·3), (00·6), (00·9) and (00·12) reflections were also measured at 223 and at 155 °K. These low temperature measurements were made using two crystals other than the one used for room temperature measurements. Both of the crystals used for the low temperature work came from the same large crystal. No significant differences between the two, with regard to dI/dT, were detected.

3. Analytic procedures

Reduction of the data to $|F|^2$ values

If the distributions of diffracting material in the specimen and of intensity in the incident beam are cylindrically symmetrical about the axis of the incident X-ray beam, the same peak height should be obtained for a given reflection regardless of the layer in which it occurs. Under these conditions, a curve of B_0 versus θ (where B_0 is the ratio of peak area to peak height) measured in the zero layer should be directly applicable for translating all peak heights (intensities), regardless of layer, into the areas (integrated intensities) that would have been measured in the zero layer. Such a curve was prepared and was applied to all peak intensities. It is shown in Fig. 1. The observed scatter indicates a probable error less than 3% due to the use of this curve.

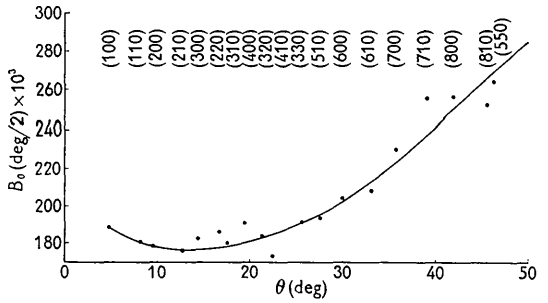

Fig. 1. Angular dependence of integral breadths, B_0.

Comparison of $|F_o|^2$ and $|F_c|^2$ after several cycles of least-squares refinements showed no trend with layer nor any systematic differences among ratios of $|F_o|^2/|F_c|^2$ for (00·l), (h0·0) and (h0·h) as would have been expected if our procedure were systematically in error.

The usual Lorentz and polarization factors for zero layer measurements were applied after the peak intensity data were reduced to equivalent zero-layer integrated intensities. Absorption corrections based on the tables of Evans & Ekstein (1952) were applied on the assumption that the specimens were perfectly spherical.

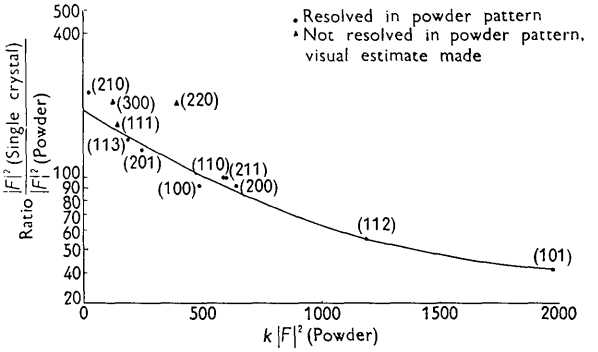

Fig. 2. Extinction correction. First plot.

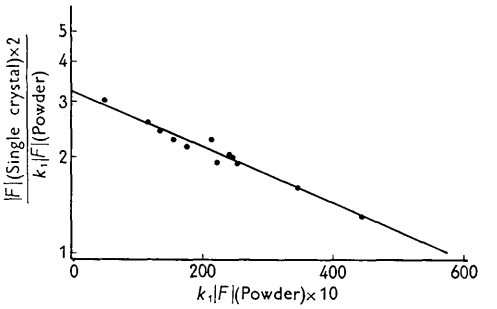

Fig. 3. Extinction correction. Second plot.

Efforts were made to correct for extinction effects by comparison of the single crystal data with powder data (also collected with filtered Mo radiation) on the assumption that the 325 mesh powder did not exhibit significant extinction effects. These data have been plotted in Figs. 2 and 3. Reasonable extremes in the the placing of the curves in Figs. 2 and 3 were explored with the result that the differences among the indicated corrections exceeded 10% only for the weakest reflections.

Extinction corrections were based on the curve shown in Fig. 4; the dashed line was given precedence over the solid line. The solid curve in Fig. 4 was obtained from Fig. 3. However, one value of $|F_o|^2$ larger than the maximum predicted by the solid line in Fig. 4 was observed at low temperatures. A curve, redrawn from Fig. 2, was therefore weighted with the solid line in Fig. 4 to give the dashed line extrapola-

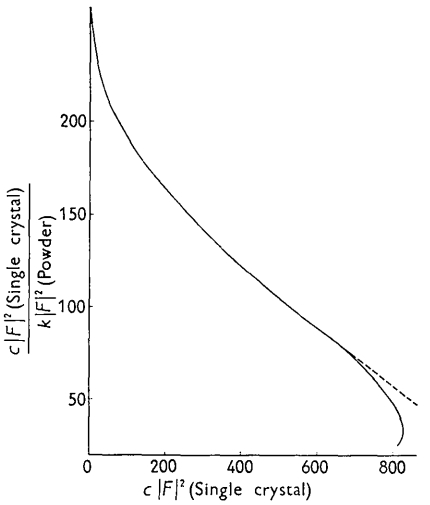

Fig. 4. Extinction correction as used.

tion shown. Comparisons of the final $|F_c|$ with $|F_o|$ indicate that the corrections were generally valid to $\pm 5\%$, except for some of the strongest reflections; the latter (12 in all) were omitted from the least-squares calculations.

Refinement procedures

The (hk·0) and (h0·l) electron density and electron density 'difference' maps were first calculated using an IBM 650 computer. Positional parameters and approximate temperature factors based on the above are summarized in Table 1 (listed under FS (hk0) and FS ($h0l$). Atomic form factors were taken from Berghuis *et al.* (1955) so far as possible.

Least-squares refinements were then computed (under the supervision of Dr William Busing) on the Oracle Computer at the Oak Ridge National Laboratory. The least-squares program of Busing & Levy (1958), which utilizes the full matrix and anisotropic temperature factors for each atom, was employed in these calculations. After three refinement cycles with the full three-dimensional (3-D) data, the weighted R factor, based on $|F|^2$, was 24%. This corresponds to about 12% for the usual R factor.

In an effort to check on the validity of the scale factors used, values of R were computed for each layer. The scale factor used for the zero layer data thereby appeared to differ most from the overall scale factor. The zero layer scale factor was therefore made a separate adjustable parameter during subsequent least-squares calculations.

Table 3. *Temperature dependence of coordinates**

Temperature	Coordinate × 10^4 x	y	z	u
300 °K.	4113	2667	1184	4698
223	4115	2682	1173	4693
155	4116	2690	1164	4686

* Based only on 2-D LS results and estimated ΔZ. Absolute accuracy is inferior to that of 3-D LS results.

Four additional refinement cycles were then com-

Table 1. *α–Quartz*

Refinement†	Coordinate parameters* × 10^4 x	y	z	u	$R(F)$	$S(F)$
At 300 °K.						
LS 3-D	4152_7	2678_6	1184_4	4705_3	8·1	0·95, 0·93
LS($h0l$)Y	4188_{19}	2685_{17}	1192_9	4706_7	13·2	0·82
LS($h0l$)B–1	4157_{15}	2690_{14}	1157_9	4707_7	11·9	0·92
LS($h0l$)B–2	4148_{13}	2689_{13}	1165_7	4706_6	13·3	0·95
FS($h0l$)	4147	2660	1173	4698		
FS(hk0)	4136	2643		4688		
LS(hk0)*a*	4113_{15}	2667_{14}		4698_6	7·0	1·07
At 223 °K.						
LS(hk0)*d*	4115_{13}	2682_{12}		4693_6	5·7	1·07
At 155 °K.						
FS(hk0)	4121	2666		4678		
LS(hk0)*e*	4116_{11}	2690_{12}		4686_6	5·6	1·07

* Subscript is standard deviation.

† LS = least-squares, FS = Fourier synthesis, Y = present work, B–1 = corresponding part of Brill data, B–2 = all data given by Brill.

Table 2. *Summary of α-quartz coordinate parameters at* 300 °K.

	x	y	z	u
Present work	0·4152 ± 0·0007	0·2678 ± 0·0006	0·1184 ± 0·0004	0·4705 ± 0·0003
Values obtained from reprocessed Brill data	0·4148 ± 0·0013	0·2689 ± 0·0013	0·1165 ± 0·0007	0·4706 ± 0·0006
Values originally reported by Brill	0·415 ± 0·003	0·272 ± 0·003	0·120 ± 0·002	0·465 ± 0·003

puted in which all reflections for which $|F_o|^2$ was >3000 (on the scale used in Table 10) were omitted. The omission of these reflections did not improve R greatly nor did it change the parameters significantly. It had been noted that omission of the 12 strongest reflections reduced R (at an early stage) from 22% to 15·2%. These 12 strongest reflections were therefore assigned zero weight in subsequent refinement cycles.

An adjustment in the general weighting scheme was also made at this point and a final sequence of four cycles was computed. The results of this last sequence of four cycles are given in Tables 1, 2, and 4. In no case did the last cycle of refinement change any parameter by more than its standard deviation. Values of $|F_o|^2$ and $|F_c|^2$ are given in Table 10.

Two-dimensional (2-D) least-squares refinements were also computed using (hk·0) and ($h0$·l) data. The (hk·0) refinements were based on the 32 independent reflections that occur within the (90·0) circle in the zero layer. The three sets of data used are shown in Table 9. The weighted $R(F)$ values were 7·0%, 6·0% and 6·2%, in that order. Parameters computed from the above are listed in Tables 3, 4, and 6.

Refinements were also carried out with two additional sets of low temperature (hk·0) data in which the $|F_o|^2$ values differed from the corresponding values in Table 9 by up to 5% as a result of applying the extinction correction in a somewhat different manner. The relative insensitivity of the final parameters to small differences in the extinction correction was demonstrated by the fact that the different methods of applying the extinction correction produced no difference in any final positional or thermal parameter greater than the standard deviation.

Four cycles of least-squares refinements were carried out on each of three sets of ($h0$·l) data as an aid in the comparison of the present work with that of Brill *et al.* (1939, 1942). Set Y was based on the ($h0$·l) data obtained in the present work. B–1 was based on corresponding reflections taken from the more extensive ($h0$·l) data of Brill. B–2 was based on the complete set of data listed by Brill. The weighting scheme was the same as that used in the third 3-D sequence except that no reflections were omitted. The results are shown in Tables 1, 2, and 4.

Table 4. *α-Quartz*

Temperature factors* at 300 °K. ($\times 10^4$) from least-squares refinements

Oxygen

Refinement†	β_{11}	β_{22}	β_{33}	β_{12}	β_{13}	β_{23}
3-D	143_{11}	81_9	90_6	85_9	-32_7	-42_5
($h0l$)Y	130_{34}	29_{28}	68_{13}	69_{25}	-31_{16}	-35_{16}
($h0l$)B–1	162_{30}	67_{24}	72_{11}	61_{23}	11_{14}	9_{14}
($h0l$)B–2	169_{24}	117_{20}	86_9	88_{18}	9_{12}	-1_{10}
($hk0$)a	166_{19}	108_{19}		96_{18}		

Silicon

Refinement†	β_{11}	β_{22}	β_{33}	β_{13}
3-D	49_4	27_5	49_3	-1_2
($h0l$)Y	12_{12}	20_{14}	28_8	2_4
($h0l$)B–1	94_{12}	75_{13}	50_6	1_4
($h0l$)B–2	100_9	89_{11}	59_5	-2_3
($hk0$)a	70_9	63_{10}		

* Subscript is standard deviation.

† Y=Present work ($h0l$), B–1=corresponding part of Brill's data, B–2=all data given by Brill *et al.*

Table 5. *Atomic thermal ellipsoids at* 300 °*K.*

Lengths in Å, angles in degrees

Silicon

	$u(1)$	$\sigma(u(1))$	$u(2)$	$\sigma(u(2))$	$u(3)$	$\sigma(u(3))$
u, length*	*0·0493*	0·0045	*0·0855*	0·0026	*0·0723*	0·0035
u_x	0·00000	0·000000	0·000000	0·000000	*0·0723*	0·0035
$u_{y'}$†	*0·0492*	0·0046	0·0056	0·0060	0·000000	0·000000
u_z	0·0032	0·0035	*0·0853*	0·0026	0·000000	0·000000
φ_x	90·00	0·00	90·00	0·00	180·00	0·00
$\varphi_{y'}$	*3·75*	4·06	93·75	4·06	90·00	0·00
φ_z	86·25	4·06	*3·75*	4·06	90·00	0·00

Oxygen

u	*0·1335*	0·0040	*0·0524*	0·0075	*0·0989*	0·0048
u_p‡	0·0032	0·0125	0·0151	0·0048	*0·0947*	0·0054
u_q	*0·1314*	0·0042	0·0083	0·0029	0·0072	0·0093
u_r	0·0231	0·0067	*0·0495*	0·0073	0·0276	0·0087
φ_p	91·4	5·4	73·3	5·2	*16·8*	5·2
φ_q	*169·9*	3·2	80·8	2·8	94·2	5·4
φ_r	100·00	2·9	*160·8*	4·5	73·8	5·3

* u is the r.m.s. amplitude of the thermal vibration, u_i is the component on the ith coordinate axis, φ_i is the angle between the ellipsoid axis of length u and the ith coordinate axis.

† y' is perpendicular to x and to z.

‡ Directions p, q, and r are given by Fig. 8(b) with q out of page.

Table 6. *Test of Debye formula for $\beta(T)$*

Temp. (°K.)	Quantity	Oxygen $\beta 11$	Oxygen $\beta 22$	Oxygen $\beta 12$	Silicon $\beta 11$	Silicon $\beta 22$
300	$\beta_o \times 10^4$	166_{19}	108_{19}	96_{18}	70_9	63_{10}
300	Debye Θ (°K.)	435	546	402	510	540
223	$\beta_c \times 10^4$	129	85	74	55	50
223	β_o* $\times 10^4$	121	81	67	56	43
223	$\beta_o \times 10^4$	126_{15}	85_{16}	70_{15}	57_8	46_9
155	$\beta_c \times 10^4$	98	67	58	43	39
155	β_o* $\times 10^4$	93	64	53	44	33
155	$\beta_o \times 10^4$	106_{14}	71_{16}	60_{14}	47_8	39_8

All 'observed' temperature factor are based on least-squares refinements of $(hk{\cdot}0)$ data.
Asterisk on β indicates difference in method of using extinction correction.
Subscripts are standard deviations.

Temperature dependence of the z-coordinate of the oxygen atom

The structure factor for $(00{\cdot}l)$ is

$$F_{00l} = 3(f_{\mathrm{Si}} \exp[-M_{\mathrm{Si}}] + 2f_{\mathrm{O}} \exp[-M_{\mathrm{O}}] \cos(2\pi lz)). \quad (1)$$

The intensities of (00·3), (00·6), (00·9), and (00·12) reflections were measured as functions of temperature over the range from 155 to 300 °K. The results of the 2-D least-squares refinements at different temperatures were used to check predictions of the low temperature values of the temperature factors on the basis of their room temperature values, using the Debye–Waller expression (James, 1954):

$$M = (6h^2/mk)(T/\Theta^2)\{\varphi(x) + x/4\} \sin^2\theta/\lambda^2. \quad (2)$$

In Table 6 we have listed temperature factors computed in the course of the least-squares refinements of the three sets of $(hk{\cdot}0)$ data (300, 223 and 155 °K.). Changes in temperature factors between room temperature and each of the two lower temperatures were then computed independently using the Debye–Waller procedure as described in detail by James, Chapter V, (James, 1954). These calculations are based on measurements of the changes of reflection intensities with temperature. The calculated changes in temperature factors were added to the room temperature factors and the results are listed in Table 6 as 'β_c'.

It is clear that the temperature dependence of the temperature factors of α-quartz in the range 155 to 300 °K. is described by the Debye–Waller formula within the standard deviations of this experiment.

Temperature factors applicable to 155 and 223 °K. were therefore calculated from equation (2) and substituted in equation (1) to allow direct solution for z. In these calculations emphasis was placed on changes in intensities rather than on their absolute values. The behavior of the (00·9) data has not been satisfactorily explained in detail; measurements of the other three reflections indicate that the z parameter of the oxygen atom changes by $-0{\cdot}0011$ from 300 to 223 °K., and by an additional 0·0009 between 223 and 155 °K.

4. Results

The electron densities projected onto the x, y plane are shown in Figs. 5 and 6 for 300 and 155 °K., respectively. In each case, one complete oxygen tetrahedron is shown about the silicon atom near the center of the figure. These maps supplement the $(h0{\cdot}l)$ projection of α-quartz published by Brill *et al.* (1942).

In order to show the dependence of results on the analytic procedures and data used, Table 1 lists the coordinate parameters obtained by each of several methods. The symbols FS and LS refer to Fourier Synthesis and Least-Squares procedures.

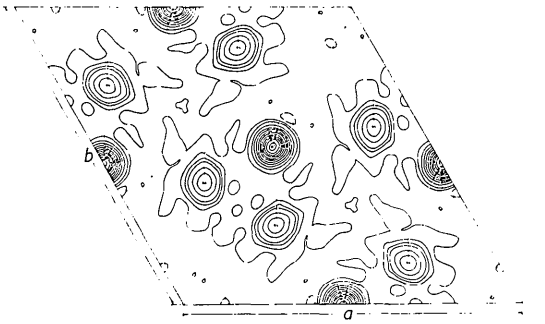

Fig. 5. Projected electron density (in e.Å^{-2}) in α-quartz at 300 °K.

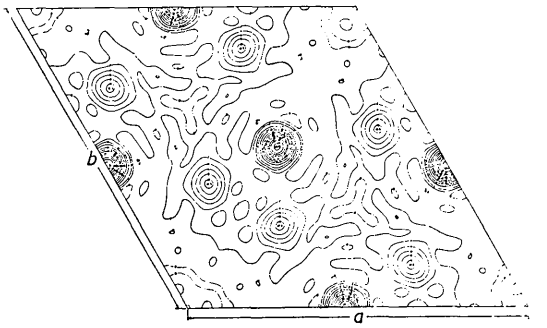

Fig. 6. Projected electron density (in e.Å^{-2}) in α-quartz at 155 °K.

The room temperature coordinate parameters which are considered to be most reliable are those obtained from the least-squares refinements of the 3-D data (Table 1, line 1). The relative insensitivity of the coordinate parameters to details of the extinction correction has been pointed out (also the 12 reflections likely to be most subject to extinction were omitted from the LS refinements). The variation in the results obtained for the oxygen x coordinate indicates that it is the least well known of the coordinate parameters.

Although Brill's reported coordinates differed slightly from ours, the results obtained from the re-refinement of the Brill data (B–2, 172 reflections) agree very well with the 3-D values obtained here.

The data used by Brill were collected from slabs of natural milk quartz, larger than the X-ray beam, with an ionization chamber; the intensity data for the present work were collected with a scintillation counter from spheroids of clear synthetic quartz small enough to be completely bathed by the X-ray beam. Consequently, those ranges of values for the coordinate parameters which include both the best values for the present material and the values obtained from re-processing the Brill data are probably representative for α-quartz.* In Table 2, the more important coordinate results have been summarized.

The FS and LS methods give essentially the same results for the temperature induced changes in the coordinates even though they give somewhat different results for the coordinate parameters themselves. Though the indicated changes are of the order of only $1\frac{1}{2}$ to 2 times the standard deviations they appear real in view of (1) the fact that the results at the intermediate temperatures are intermediate between the results for the two extreme temperatures, and (2) the fact that the temperature induced *changes* in intensities were the quantities experimentally obtained and used to deduce the low temperature from the observed room temperature structure factors. Thus the standard deviations at each low temperature are expected to be due more to the uncertainty in the room temperature results than to uncertainties in the temperature-induced changes. One full set of 2-D LS coordinates and the calculated z coordinates for each temperature (determined from the 3-D room temperature result and the previously calculated change in z) are re-tabulated in Table 3 without the standard deviations and other results shown in Table 1.

The temperature factors obtained from the least-squares refinements of various sets of 300 °K. data are listed in Table 4. The differences among the three sets of $\{h0\cdot l\}$ results seem to indicate that the mean square displacements (whether or not of wholly thermal origin) of the silicon atom parallel to the two-fold axis were larger in the milk quartz used by Brill than in the clear synthetic quartz used in the present work. However, the positional parameters are essentially the same both for Brill's crystals and for the present ones.*

The principal axes of the individual thermal ellipsoids were arbitrarily numbered 1, 2, and 3. The components, u_i, of each of these axes in the direction of the ith coordinate axis and the angles, φ_1, between the principal axes of the ellipsoids and the ith coordinate axis, were calculated from the 3-D temperature factors and are listed in Table 5. The principal features of the thermal ellipsoids are presented in Figs. 7 and 8. In Fig. 7 the x-axis is a two-fold axis in the crystal, and the y'-axis is perpendicular to the two-fold and the three-fold axes. Principal axes of the silicon ellipsoid are parallel to these directions in the crystal. The largest amplitude of vibration of the silicon atom is along the three-fold axis and the direction of smallest thermal motion is perpendicular to both the three-fold and the two-fold axes.

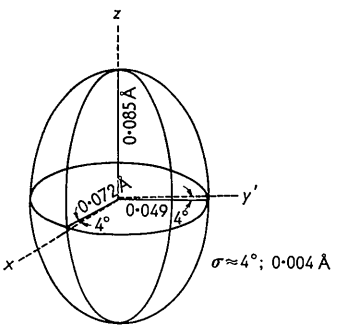

Fig. 7. Thermal ellipsoid of silicon in α-quartz at 300 °K.

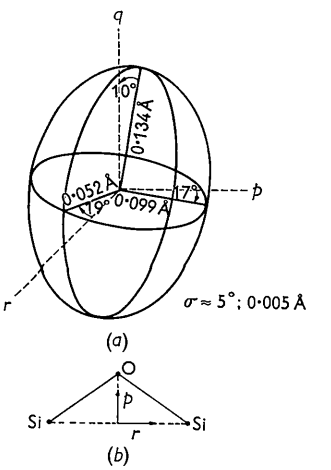

Fig. 8. Thermal ellipsoid of oxygen in α-quartz at 300°K. (*a*) Ellipsoid. (*b*) Axes to which ellipsoid is referred.

* Since this work was completed, Smith & Alexander (1960) have reported on the results of refinement by differential synthesis methods of their very careful counter data obtained with Cu $K\alpha$ radiation from clear, natural crystals ground to small spheres. They have made a detailed point by point comparison of their results with ours (at 300 °K.) and found that their positional parameters agree very well with our 3-D results. Discrepancies between the 2 sets of results did not exceed the standard deviations in any case.

* And also for the Smith & Alexander (1960) crystals.

In Table 5 the orientation of the oxygen thermal ellipsoid is referred to two coordinate systems, the $xy'z$ system defined as above the pqr system described in Fig. 8(b), in which the axes are defined in the relation to the Si–O–Si group. It appears that the deviation of the ellipsoid orientation from its simply expected orientation may be real.

The electron density maps shown in Figs. 5 and 6 are based on phase angles determined by least-squares procedures. Fig. 9 shows the result of subtracting the 155 °K. map from the 300 °K. map. Since the changes in atomic coordinates were no larger than 0·002, (between 155 and 300 °K.) this map should reflect principally the differences in the thermal vibrations at the two temperatures. These differences give rise to the negative regions at the atomic positions. Anisotropy in the thermal motions is indicated by the anisotropic increase of electron density about the atomic positions with increasing temperature. This increase is expected to be centrosymmetric about the atomic position. The rather pronounced lack of this centrosymmetric character in the increase about the silicon appears to be due to the slight change of the atomic position with temperature.

The room temperature interatomic angles and distances are listed in Table 7. The small differences among 'equivalent' bond angles and distances indicate that the SiO_4 tetrahedron is slightly distorted. The magnitude of the indicated distortion from the regular tetrahedron is 2 to 3 standard deviations.

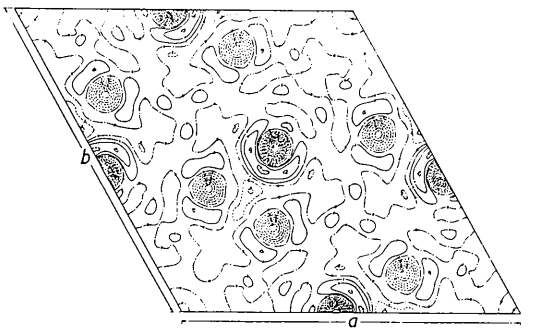

Fig. 9. α-Quartz (300 − 155 °K.) temperature difference map. ——— Positive, – – · – negative, electron density in e.Å^{-2}.

Table 7. *α-Quartz*

Interatomic distances and angles at 300 °K.

Angles (°)

O–Si–O		Si–O–Si		Dihedral	
Angle	σ	Angle	σ	Angle	σ
108·74	0·05	143·90	0·19	89·05	0·11
109·16	0·22			89·40	0·16
110·04	0·22			90·34	0·25
110·08	0·17				

Lengths (Å)

Si–O		O–O		Si–Si	
Distance	σ	Distance	σ	Distance	σ
1·603	0·003	2·635	0·004	3·0565	0·0002
1·611	0·002	2·613	0·005		
		2·613	0·002		
		2·613	0·002		
		2·641	0·005		

Table 9. *Observed and calculated (hk·0) structure factors at 300 °K.*

	Case *a*, 300 °K.		Case *d*, 223 °K.		Case *e*, 155 °K.	
hk	$\|F_o\|^2$	$\|F_c\|^2$	$\|F_o\|^2$	$\|F_c\|^2$	$\|F_o\|^2$	$\|F_c\|^2$
10	1683	2238	1707	2090	1741	2101
20	2842	2863	2891	2957	2984	2998
30	742	671	711	631	682	610
40	1915	1477	1884	1489	1871	1468
50	24	1	26	1	28	1
60	196	198	186	187	171	174
70	309	317	406	418	502	510
80	124	144	151	167	160	175
90	9	1	11	2	13	2
11	2848	3257	2960	3368	3062	3414
21	126	127	132	129	137	136
31	7045	3368	7450	3561	7703	3730
41	111	132	121	140	125	148
51	425	414	465	456	504	491
61	709	678	765	745	843	809
71	357	349	419	423	471	475
81	164	165	240	234	297	289
22	6621	3570	6681	3568	6816	3559
32	1295	1071	1430	1156	1527	1216
42	1948	1409	2150	1553	2258	1618
52	4	10	11	16	13	20
62	55	61	54	66	54	65
72	4	1	4	1	2	1
33	1627	1244	1893	1429	2087	1579
43	72	84	73	87	78	91
53	329	337	354	368	388	396
63	103	131	134	157	163	185
73	170	157	207	186	229	209
44	198	213	259	269	285	299
54	11	16	13	16	16	17
64	64	63	72	73	78	80
55	705	603	908	793	1112	951

Table 8. *Effect of temperature on interatomic distances*

Based on least-squares (hk·0) results and room temperature thermal expansion coefficients

Temp.	Angles (°)		Distances (Å)*				
			Si–O		O–O		
(°K.)	Si–O–Si	Si–Si	I–1	I–3	I–3	1–4	6–3
300	143·0°	3·0573	1·608	1·615	2·656	2·605	2·627
223	142·7°	3·0545	1·609	1·616	2·656	2·608	2·632
155	142·5°	3·0524	1·607	1·617	2·655	2·608	2·633

* *Absolute* accuracy inferior to 3-D least-squares results at 300 °K.

The effect of temperature on the bond distances and angles was investigated by computing distances based on the coordinates listed in Table 3. The results, listed in Table 8, are believed to reflect the temperature dependence of the bond lengths accurately but do not represent the best absolute values of the lengths at anyone temperature.

The Si–O and O–O nearest neighbor distances show no consistent trends with temperature. The two Si–O bond distances differ by about two standard deviations at room temperature. Libration of the oxygen atom would increase the differences. The same is true of the O–O distances in the tetrahedron. The apparent distortion of the tetrahedron, which is indicated by the dihedral angles as well as by the bond angles and distances, either remained unchanged or increased

Table 10. *Observed and calculated (hk·l) structure amplitudes at* 300 °*K*.*

	$l=0$		$l=1$		$l=\bar{1}$		$l=2$		$l=\bar{2}$	
hk	$\lvert F_o\rvert^2$	$\lvert F_c\rvert^2$	$\lvert F_o\rvert^2$	$\lvert F_c\rvert^2$	$\lvert F_o\rvert^2$	$\lvert F_c\rvert^2$	$\lvert F_o\rvert^2$	$\lvert F_c\rvert^2$	$\lvert F_o\rvert^2$	$\lvert F_c\rvert^2$
00	—	—	—	—	—	—	—	—	—	—
10	2136	2220	5340	5746	12301	13747	1702	2787	624	709
20	3598	2969	1624	1726	820	694	816	734	2699	3247
30	940	776	478	3	14254	7901	5387	4580	2225	2107
40	2424	1756	3921	2837	525	321	108	64	822	827
50	31	0	58	51	382	405	9940	3884	289	21
60	248	291	1140	940	208	98	482	519	286	267
70	391	439	85	28	1055	1033	260	286	21	3
11	3606	3087	874	914	874	914	4676	5575	4676	5575
21	160	120	3469	2985	4017	3376	1368	1266	3725	3946
31	8921	3566	919	660	2215	1906	1458	1224	3647	2901
41	141	148	2892	2074	470	289	484	442	734	703
51	538	490	1673	1281	126	41	103	110	449	454
61	898	797	196	209	233	251	155	111	1049	981
71	452	474	117	121	161	190	12	19	35	47
22	8384	3764	1189	1034	1189	1034	21	33	21	33
32	1640	1110	177	33	3653	2576	942	946	132	98
42	2466	1651	190	178	420	375	312	253	1358	1151
52	6	6	143	72	1973	1539	1154	1006	422	360
62	69	99	318	311	367	368	97	101	377	403
33	2061	1418	1078	906	1078	906	35	55	35	55
43	91	116	939	856	659	590	175	138	1076	1031
53	416	424	3	5	12	14	225	290	167	174
44	251	312	105	114	105	114	443	451	443	451
54	14	121	163	160	406	424	—	—	—	—

* All values are based on $F_{000}=90$ and have been multiplied by 10.

	$l=3$		$l=\bar{3}$		$l=4$		$l=\bar{4}$		$l=5$	
hk	$\lvert F_o\rvert^2$	$\lvert F_c\rvert^2$	$\lvert F_o\rvert^2$	$\lvert F_c\rvert^2$	$\lvert F_o\rvert^2$	$\lvert F_c\rvert^2$	$\lvert F_o\rvert^2$	$\lvert F_c\rvert^2$	$\lvert F_o\rvert^2$	$\lvert F_c\rvert^2$
00	507	933	—	—	—	—	—	—	—	—
10	105	14	1105	1838	2574	3549	904	1084	1044	1089
20	12972	9513	2740	2777	493	600	44	16	17	2
30	522	591	111	71	326	338	618	740	466	570
40	3253	2335	1696	1392	41	9	321	347	222	214
50	47	70	6	1	152	31	2318	1862	919	894
60	254	243	1067	984	406	462	35	117	29	10
70	23	15	6	8	33	2	536	548	—	—
11	1032	1280	1044	1280	2554	3000	2554	3000	1158	1380
21	2554	2766	726	726	1936	2180	196	105	198	161
31	410	437	519	519	906	954	365	344	312	326
41	301	214	2355	2355	1239	1187	157	118	87	52
51	1364	1160	840	840	41	37	365	418	297	337
61	120	136	134	134	312	345	97	92	29	56
71	—	—	—	—	—	—	—	—	—	—
22	2213	2077	2213	2213	709	734	709	734	807	786
32	6	6	12	12	540	417	2921	2453	2516	2050
42	499	534	621	621	540	532	283	269	181	189
52	105	113	37	37	76	75	225	250	268	292
62	274	328	155	155	278	316	21	3	—	—
33	930	841	930	930	402	395	402	395	361	349
43	388	407	114	114	540	521	58	40	47	36
53	1067	986	336	336	140	192	15	6	—	—
44	301	350	301	301	225	216	225	216	—	—
54	—	—	—	—	—	—	—	—	—	—

Table 10. (*cont.*)

	$l=\bar{5}$		$l=6$		$l=\bar{6}$		$l=7$		$l=\bar{7}$	
hk	$\lvert F_o\rvert^2$	$\lvert F_c\rvert^2$	$\lvert F_o\rvert^2$	$\lvert F_c\rvert^2$	$\lvert F_o\rvert^2$	$\lvert F_c\rvert^2$	$\lvert F_o\rvert^2$	$\lvert F_c\rvert^2$	$\lvert F_o\rvert^2$	$\lvert F_c\rvert^2$
00	—	—	1364	1478	—	—	—	—	—	—
10	2565	2987	490	572	41	3	64	12	770	827
20	120	170	790	736	3055	2781	198	226	152	141
30	68	59	29	9	301	325	262	222	1216	1045
40	27	2	552	526	979	915	429	412	27	1
50	117	76	15	10	6	5	47	1	904	818
60	528	516	466	432	82	56	—	—	—	—
70	—	—	—	—	—	—	—	—	—	—
11	1158	1380	326	365	326	365	569	597	569	597
21	1304	1503	161	113	674	747	711	695	379	371
31	583	660	365	367	262	262	653	631	225	216
41	1032	1033	880	834	73	28	181	190	149	143
51	56	50	202	206	534	524	219	218	27	15
61	172	184	—	—	—	—	—	—	—	—
71	—	—	—	—	—	—	—	—	—	—
22	807	786	1053	988	1053	988	9	9	9	9
32	426	296	47	56	27	30	23	16	167	180
42	196	203	373	387	256	255	213	205	76	68
52	38	20	3	9	41	52	—	—	—	—
62	—	—	—	—	—	—	—	—	—	—
33	361	349	309	290	309	290	12	3	12	3
43	297	303	38	33	189	205	—	—	—	—
53	—	—	—	—	—	—	—	—	—	—
44	—	—	—	—	—	—	—	—	—	—
54	—	—	—	—	—	—	—	—	—	—

	$l=8$		$l=\bar{8}$		$l=9$		$l=\bar{9}$	
hk	$\lvert F_o\rvert^2$	$\lvert F_c\rvert^2$	$\lvert F_o\rvert^2$	$\lvert F_c\rvert^2$	$\lvert F_o\rvert^2$	$\lvert F_c\rvert^2$	$\lvert F_o\rvert^2$	$\lvert F_c\rvert^2$
00	—	—	—	—	1778	1230	—	—
10	921	823	242	183	73	43	138	119
20	68	77	12	13	478	423	215	180
30	1123	960	79	16	91	92	21	10
40	62	42	546	514	—	—	—	—
50	—	—	—	—	—	—	—	—
60	—	—	—	—	—	—	—	—
70	—	—	—	—	—	—	—	—
11	163	161	163	161	105	92	105	92
21	350	351	321	321	23	24	3	1
31	146	183	114	115	—	—	—	—
41	82	70	278	278	—	—	—	—
51	—	—	—	—	—	—	—	—
61	—	—	—	—	—	—	—	—
71	—	—	—	—	—	—	—	—
22	58	58	58	58	—	—	—	—
32	260	254	17	1	—	—	—	—
42	—	—	—	—	—	—	—	—
52	—	—	—	—	—	—	—	—
62	—	—	—	—	—	—	—	—
33	—	—	—	—	—	—	—	—
43	—	—	—	—	—	—	—	—
53	—	—	—	—	—	—	—	—
44	—	—	—	—	—	—	—	—
54	—	—	—	—	—	—	—	—

with decreasing temperature, and does not appear to be of thermal origin.

The internal consistency of the coordinate results obtained by using different refinement procedures and the agreement of our coordinate results with those obtained by reprocessing the data of Brill *et al.*, which were gathered from a different type of quartz crystal, have made it possible to report improved coordinate values for α-quartz. Real specimen-to-specimen differences have been noted, particularly in the temperature factors. The scale factor reported by Brill *et al.*, which had been determined by direct measurement, was changed slightly when left as a variable in the least-squares refinement of their data.

An (F_o-F_c) difference map based on the 155 °K. LS results is shown in Fig. 10. The 155 °K. data were chosen in order to minimize errors due to incorrect temperature factors. The R factor for the 2-D LS refinement on which Fig. 10 is based was 5·6%. Thirty independent reflections were used. The (310)

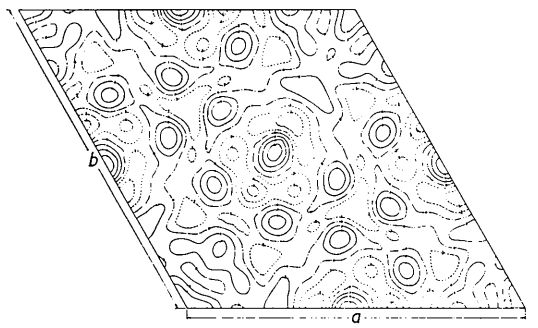

Fig. 10. α-Quartz ($F_o - F_c$) difference map at 155 °K. ——— Positive, - - - - negative, electron density in e.Å^{-2}.

and (220) reflections were omitted from the LS refinement and the difference map of Fig. 10. There are significantly large regions of negative and positive density in this map indicating that a relatively low R factor in the LS refinement does not necessarily mean that further adjustments may not be indicated by a difference map.

We are particularly grateful to Dr William R. Busing of the Oak Ridge National Laboratory for his services in providing us with all of the ORACLE computer results based on our data. We also wish to express our appreciation to the Georgia Institute of Technology for the donation of many hours of computer time (IBM 650) and to the staff of the Georgia Institute of Technology Computer Center for their aid in using the computer. We are pleased to thank Prof. I. Fankuchen of the Polytechnic Institute of Brooklyn for helpful discussions.

References

BERGHUIS, J., HAANAPPEL, IJ. M., POTTERS, M., LOOPSTRA, B. O., MACGILLAVRY, C. H. & VEENENDAAL, A. L. (1955). *Acta Cryst.* **8**, 478.

BRADLEY, W. F. & JAY, A. H. (1933). *Proc. Roy. Soc.* A, **142**, 507.

BRILL, R., HERMANN, C. & PETERS, CL. (1939). *Naturwiss.* **27**, 676.

BRILL, R., HERMANN, C. & PETERS, CL. (1942). *Ann. Phys.* **41**, 233.

BUSING, W. H. & LEVY, H. A. (1958). Paper G-4 at the June 23–27 American Crystallographic Association Meeting in Milwaukee.

EVANS, H. T. & EKSTEIN, M. (1952). *Acta Cryst.* **5**, 540.

JAMES, R. W. (1954). *The Optical Principles of X-Ray Diffraction.* London: Bell.

POST, B., SCHWARTZ, R. S. & FANKUCHEN, I. (1951). *Rev. Sci. Instrum.* **22**, 218.

SMITH, G. S. & ALEXANDER, L. A. (1960). Paper E-8 at the January 25–27 American Crystallographic Association Meeting in Washington, D.C.

Acta Cryst. (1962). **15**, 346

X-ray Studies of Molecular Overcrowding. III. The Crystal and Molecular Structure of *o*-Bromobenzoic Acid.

BY G. FERGUSON AND G. A. SIM

Chemistry Department, The University, Glasgow, W. 2, Scotland

(*Received* 16 *May* 1961)

o-Bromobenzoic acid crystallizes in the monoclinic system, space group $C2/c$, with eight molecules in a unit cell of dimensions

$$a = 14{\cdot}82,\ b = 4{\cdot}10,\ c = 25{\cdot}90\ \text{Å};\ \beta = 118°\ 15'.$$

The final atomic coordinates were obtained from a three-dimensional least-squares refinement involving 1145 observed structure factors. The molecules occur as centrosymmetrical dimers with hydrogen bonds (2·64 Å) between adjacent carboxyl groups. The strain which would be imposed on an ideal planar molecule is relieved in a number of ways.

(i) The carboxyl group is rotated about the exocyclic carbon–carbon bond 18·3° out of the plane of the benzene ring.

(ii) The exocyclic substituents are deflected in opposite directions out of the aromatic plane, the bromine atom by +0·064 Å and the exocyclic carbon atom by −0·057 Å.

(iii) The exocyclic carbon–carbon and carbon–bromine bonds are displaced sideways so that the normal valency angles of 120° are increased to 123·4° and 124·9°, respectively.

1. Introduction

The previous paper in this series (Ferguson & Sim, 1961) gave a description of the molecular structure of *o*-chlorobenzoic acid in the solid state. Consideration of atomic sizes suggests that marked deviations from planarity should also occur in the molecule of *o*-bromobenzoic acid. A detailed structure analysis of this